[Research Paper] 대한금속 · 재료학회지 (*Korean J. Met. Mater.*), Vol. 60, No. 9 (2022) pp.685-693
DOI: 10.3365/KJMM.2022.60.9.685

Effects of Fillers on the Hydration Behaviors of Tricalcium Silicate Scaffolds Fabricated by Fused Deposition Modeling

Yeongjin Koo[1,2], Yoonjoo Lee[1,*], Myung-Hyun Lee[1], and Seog Young Yoon[2,†]

[1]*Energy and Environmental Division, Korea Institute of Ceramic Engineering and Technology, Gyeongsangnam-do 52851, Republic of Korea.*
[2]*Department of Materials Science and Engineering, Pusan National University, Busan 46241, Republic of Korea.*

Abstract: With the development of additive manufacturing technology, many types of materials are being utilized, and methods of printing the materials and characteristics of their hydration properties are being studied in the fields of construction and biotechnology. Tricalcium silicate (C3S), which is used as a cement material or biomaterial, is a representative hydraulic material. In previous research, scaffolds were printed via fused deposition modeling and the deformation properties during the hydration process of the printed scaffold were investigated. C3S, like ceramic materials, requires post-processing such as curing after printing, and volumetric deformation occurs during this process. Deformation information is very important to ensure the numerical value of the final product, as well as to suppress the possibility of deformation. In this study, silica, hydroxyapatite (HA), and alumina were mixed with three types of fillers to print a C3S support, which was then cured through a two-step process. In this process, HA and silica, which have good hydrophilicity, exhibited high strength due to the suppression of scaffold deformation. It was confirmed that the smaller the particle size, the more effective it was in obtaining a stable hydrated print.

(Received 10 May, 2022; Accepted 7 July, 2022)

Keywords: 3D printing, additive manufacturing, sintering-free, hydration reaction, tricalcium silicate(C3S)

1. INTRODUCTION

Additive manufacturing (AM) is a relatively simple process and is expected to be suitable for small-quantity batch production and the fabrication of objects with fine structures. With the development of 3D printing technology, research on the application of ceramic printed materials has also attracted attention. However, ceramic materials require sintering or curing after printing, which changes the size or shape of the print. Therefore, in the development of ceramic 3D printing technology, it is necessary to study the sintering and hardening behaviors of ceramic materials that occur during post-processing along with the printing technology.

Calcium silicate is a representative hydraulic material that is primarily used for construction and biological applications. In hydraulic materials such as calcium silicate, factors that can affect the hydration reaction, such as the pH, particle size, and mixing ratio [1-3], as well as phase change, density, and shape changes occurring during hydration, have been studied [3-5]. With the development of AM technology, hydraulic materials have attracted attention as candidates for 3D printing. In one such study, Yang et al printed a Ca_3SiO_5 bone cement scaffold using a biodegradable binder and investigated the surface changes of the scaffold over a long period of time [5]. In addition, Wu et al confirmed the printable time of a silica gel and tricalcium silicate mixture and described the biodegradation behavior of this scaffold [6]. Further, Pei et al compared the strength change behaviors of calcium sulfate hemihydrate cement scaffolds under a hydration atmosphere and time course [7]. Such studies make it clear that, when developing printing technology for hydraulic materials, it is necessary to blend materials suitable for printing and hydration processes and to consider various problems occurring during the hydration process.

In a previous report, two-step 3D printing method for

- 구영진: 학생연구원, 이윤주: 책임기술원, 이명현: 수석연구원, 윤석영: 교수
**Corresponding Author:* Yoonjoo Lee
[Tel: +82-55-792-2611, E-mail: yoonjoo_lee@kicet.re.kr]
†*Corresponding Author:* Seog Young Yoon
[Tel: +82-51-510-3226, E-mail: syy3@pusan.ac.kr]

hydraulic materials consisting of printing and hydration as well as the formulation of a suitable printing paste for this method were presented [8]. This process was accompanied by expansion deformation of the printed material in the hydration step for hardening, and the expansion rate and strength of the hydrate changed according to the tricalcium silicate (C3S) and tricalcium aluminate (C3A) mixing ratio. In this case, the expansion was suppressed by the combination of two materials with different reaction rates and mechanical properties; however, the key factors that could stabilize the size were not investigated in detail. Therefore, in this study, the effect of fillers on the shape deformation of printed materials composed of C3S using silica, hydroxyl apatite (HA), and alumina was evaluated to investigate the factors that inhibit the expansion deformation of the hydrate.

2. EXPERIMENTAL

2.1 Materials

$CaCO_3$ (99.9%, Kojundo Chemical Co. Ltd., Japan) and SiO_2 (99.9%, Kojundo Chemical Co. Ltd., Japan) were used as the starting materials for the preparation of C_3S ($3CaO{\cdot}SiO_2$). SiO_2 and $CaCO_3$ were mixed at a molar ratio of 1:3 with water to form a spherical shape. The mixture was heated to 1600 °C and converted into C3S via heat treatment at this temperature. The synthesized C3S was sieved through a 325 mesh after milling. Silica, HA (99.9%, Sun Medical, Republic of Korea), and alumina (99.9%, Denka, Republic of Korea) were used as filler materials, all of which were commercialized products with particle diameters of approximately 300 nm. For the silica filler, three types of spherical silica with different sizes of Sukgyung AT products were utilized (99.9%; Sukgyung AT, Republic of Korea).

Water-miscible hydrophilic oils were employed to prevent C3S from being hydrated during the printing process and to allow water to diffuse when the print was immersed in water. The oils used as media or binders were polypropylene glycol (PPG; P400, Sigma-Aldrich, USA) and polyethylene glycol (PEG; tested according to Ph. Eur., 1,000, Sigma-Aldrich, USA). The printing paste was prepared such that the powder constituted 46 vol% of the paste and the filler comprised 10% of the total volume. Even if the amount of powder is constant, the viscosity of the paste changes depending on the particle size and shape, and the extruded filament is greatly affected by the viscosity. Therefore, the amount of PPG to PEG was adjusted so that the viscosity of the paste was 5×10^3 - 10 Pa·s in the range of shear rate 0.1 - 100/s by the parallel plate method of a rotational viscometer. Other experimental details followed previous studies [8].

2.2 Printing scaffolds

The FDM printing method using an INVIVO premium printer (Rokit Healthcare, Republic of Korea) was selected. The prepared paste was filled into a syringe equipped with a 400-μm-diameter nozzle, and printing was performed at an extrusion rate of 2.0%, a nozzle movement speed of 25 mm/s, and a stacking interval of 400 μm. Creator K (STL to G-code conversion program supplied by Rokit Healthcare) was used, and the scaffold was modeled in a 40% infill mode in a 10×10×10 (mm) cube without setting the outer wall. The print was hardened via two steps: pre-hardening was performed by immersing the print in a 0.05M H_3PO_4 solution for 30 min, and then the sample was immersed in distilled water for 18 h. The hydrated scaffolds were dried at 60 °C after rinsing with distilled water.

2.3 Analysis

The phase change of the raw material was confirmed using an X-ray diffractometer (Dmax-2200, Rigaku, Japan). The diffraction patterns were measured at a scan rate of 5/min at 40 mA and 40 kV using a Cu Kα target. The particle size distributions of all powders were checked using a laser scattering particle size distribution analyzer (Horiba, Japan). The density and pore size distribution of the hydrated scaffold were measured at 30,000 psi using a mercury porosimeter (Autopore IV 9500, Micromeritics, USA), and the microstructure was observed via optical microscopy (DMX1200F, Nikon, Japan) and scanning electron microscopy (SEM; JSM-6700F, Jeol, Japan).

3. RESULTS AND DISCUSSION

3.1 Hardening of C3S printout

The synthetic C3S powder used in this study showed a bimodal distribution, in which particles of approximately 200

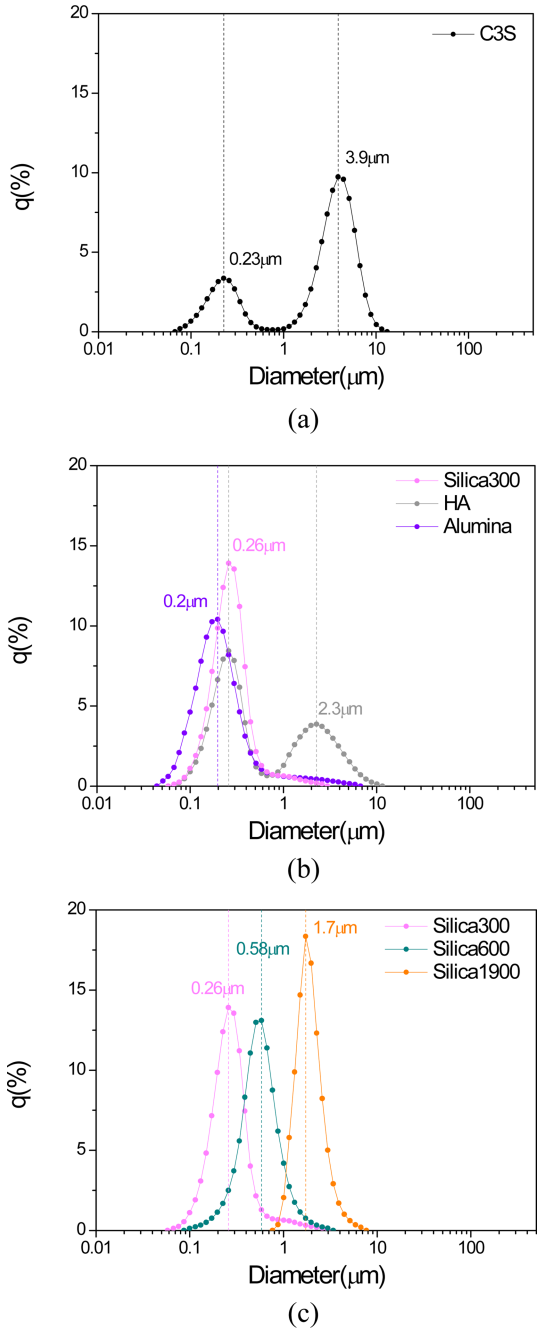

Fig. 1. Particle size distribution analysis results for (a) C3S, (b) different types of fillers with 300 nm particle diameters, and (c) silica fillers of different sizes

nm and 4 μm were mixed in a ratio of approximately 1:2 (Fig. 1(a)). Silica, HA, and alumina, which were used as fillers, were selected to have similar particle sizes. As summarized in Table 1 and Fig.1, these three powders have particle sizes of approximately 300 nm. In the case of HA, aggregated particles were directly observed in the analysis

Table 1. Particle size analysis results (nm)

Material	Mean size	Median size	Mode size
C3S	3000	3000	3700
Silica300	**300**	250	240
Silica600	600	520	540
Silica1900	1900	1700	1600
HA	1200	**300**	2400
Alumina	**300**	180	180

results, as the average particle diameter was 1200 nm, but the primary particles were 300 nm in diameter.

Figure 2(a) shows the dispersion of the extruded C3S paste in water. Because it took at least 12 h for C3S to harden completely, dispersion occurred faster than the hydration rate of C3S paste in water condition. In previous studies, it was possible to obtain well-cured scaffolds while maintaining the printed shape by incorporating C3A [8]. C3A, which has a relatively fast reaction rate, can induce the initial quick curing of the printed material; for this reason, it has been suggested that C3A can effectively maintain the structure's shape and prevent deformation until the C3S is completely cured. However, the inert silica, HA, and alumina fillers used in this study did not show any ability to prevent C3S from dispersing (Fig. 2(b)).

According to previous research, the main factor that enables curing with minimal change in shape is the reaction rate. For example, changing the concentrations of the reactants or products is the simplest means of controlling the reaction rate. As shown in the reaction equation below, C3S generates $Ca(OH)_2$ during hydration:

$$2(3CaO{\cdot}SiO_2) + 6H_2O \rightarrow 3CaO{\cdot}2SiO{\cdot}3H_2O + 3Ca(OH)_2.$$

Theoretically, decreasing the $Ca(OH)_2$ concentration can increase the forward reaction rate. Therefore, the print mixed with the filler was supported in a 0.05 M aqueous phosphoric acid solution, and it was observed that the paste was not dispersed and the scaffold shape was maintained. However, even in this case, when the sample was exposed to an acidic solution, corrosion occurred simultaneously with hydration (Fig. 2(c)).

Therefore, in this study, the curing process was divided into two steps. In the initial curing step, the print was immersed in a 0.05 M phosphoric acid solution for

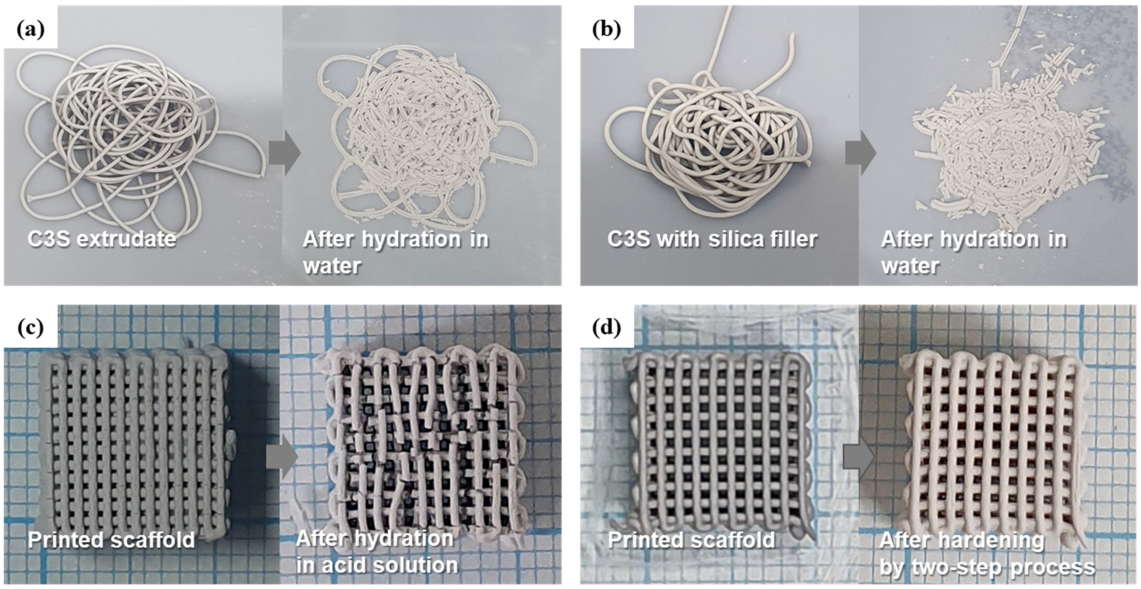

Fig. 2. Shape changes of C3S extrudate between before and after hydration under different conditions: (a) C3S mixture in water, (b) C3S with silica filler in water, (c) C3S mixed with silica in 0.05 M H_3PO_4, and (d) two-step hardening, where each hydrate was placed on the right size of the extrudate

approximately 30 min to induce a quick reaction to maintain the shape, and then the sample was transferred to distilled water to complete the hydration reaction. As shown in Fig. 2(d), it was possible to obtain a hydrate that maintained the shape of the printed scaffold structure.

3.2 Expansion behaviors and strengths of hydrate scaffolds with different types of filler materials

Because an uncured printout is a very soft paste, it is difficult to measure its size. Therefore, its size was estimated as follows. Firstly, it was confirmed that the diameter of the filament extruded from the 400 μm nozzle was 480 μm (Fig. 3(a)). As the nozzle path moved in the modeling direction (Fig. 4(a)), the cross-sectional dimensions of the print on the x-y plane were 10.38×10.38 (mm) (Fig. 4(b)). The height of the model with an interlayer thickness of 400 μm was 9.9 mm, and considering that the diameter of the extruded product was 480 μm, the thickness of the print was approximately 10.34 mm. Therefore, the dimensions of the printed scaffold were expected to be 10.38×10.38×10.34 (mm).

The hydration reaction involves a change in print size. Because C3S absorbs water molecules, expansion

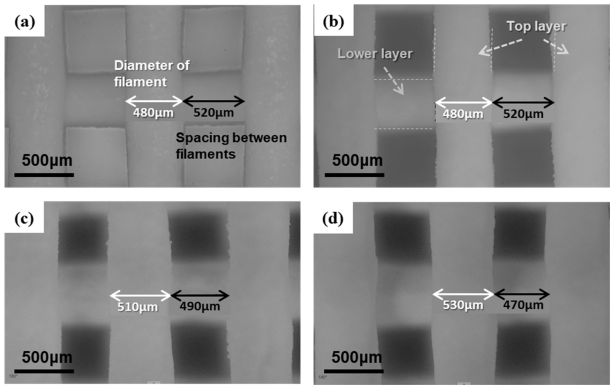

Fig. 3. Optical microscopy image of top side (x-y plane) of scaffold to compare (a) the skeleton of the printout and that of hydrates with different types of fillers: (b) silica with 300 nm diameter, (c) HA, and (d) alumina

deformation occurs and a change in the size of the scaffold itself is observed. In addition, the expansion behavior affects the change in the thickness of the skeleton forming the scaffold. In the previous results, the size in the z-direction showed a relatively small expansion rate compared with those in the x- and y-directions [8]. Table 2 summarizes the size deformation behavior of the hydrates obtained in this study along with the types of fillers.

These results also indicate that the deformations in the x- and y-directions are larger than that in the z-direction. In particular, the scaffold hydrate prepared by mixing the

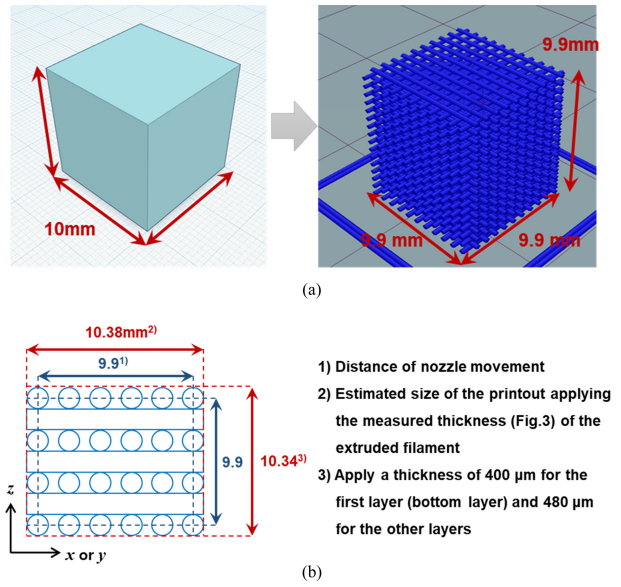

Fig. 4. (a) Modeling scaffold with 40% infill mode in the space of a 10×10×10 mm cube and (b) estimated size of the printed scaffold

Table 2 Size of scaffold hydrate with expansion rate

Filler material	Measurement(mm)		Expansion rate(%)	
	x-, *y*-axis	Height(*z*-)	*x*-, *y*-axis	Height(*z*-)
Silica300	10.39±0.09	10.25±0.01	0.10	-0.87
Silica600	10.45±0.08	10.3±0.0.3	0.67	-0.38
Silica1900	10.63±0.05	10.41±0.03	2.42	0.67
HA	10.72±0.05	10.43±0.02	3.28	0.87
Alumina	11.06±0.02	10.52±0.01	6.55	1.74

The estimated size of printed scaffold was 10.38×10.38×10.34(*h*)mm, but the height was measured lower than the model size due to the load of layers.

silica filler was measured to have dimensions of 10.39×10.39×10.25 (mm), corresponding to a change of 0.1% or less. Considering that the skeleton diameter of this specimen was maintained at 480 μm, it can be said that there was little change in the size of the silica filler (Fig. 4(b)). On the other hand, for the HA and alumina, the size of the hydrate increased by 3.28% and 6.55%, respectively. The expansion rate of the scaffold was the greatest under the condition in which the alumina filler was used, and the width of its skeleton expanded to 530 μm, representing a change of over 10% (Table 2, Figs. 3(c) and (d)).

The hydration reaction affects not only the change in size of the scaffold but also its mechanical properties, such as the compressive strengths of the hydrates, which are shown in

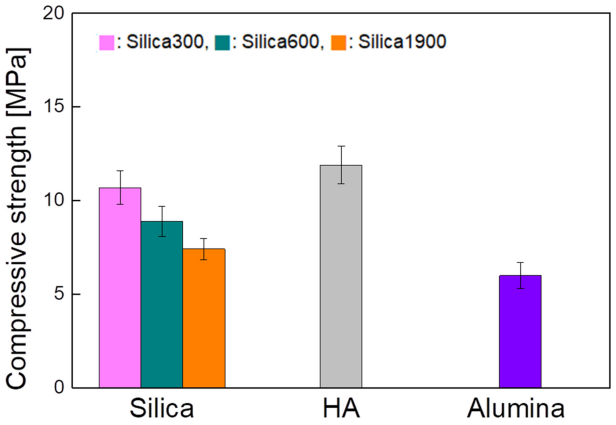

Fig. 5. Compressive strength of hydrated scaffold according to filler type and size

Fig. 5. The strength values of the scaffolds do not coincide with their expansion behaviors, but do exhibit similar tendencies. Specifically, the compressive strength under both silica and HA conditions, where the size change is less than 4%, is >10 MPa, but that of alumina, which expands by >6%, is only 6 MPa.

3.3 Scaffold microstructure

The mechanical properties of a material are also determined by the properties of the material itself, but the various factors, such as the phase, density, and microstructure, act in a complex manner. Firstly, X-ray diffraction analysis was performed to confirm the reactivity of the filler along with the hydration reaction of C3S. As mentioned in the previous section, C3S not only absorbs water molecules during hydration, but also forms $Ca(OH)_2$ crystals, so the reactivity of C3S can be confirmed by the generation of $Ca(OH)_2$. Comparing the diffraction patterns before and after hydration, the peaks at 32.2° and 41.3°, representing C3S, decreased, and the peak corresponding to the (001) plane of $Ca(OH)_2$ increased significantly (Fig. 6). Except for the relatively large $Ca(OH)_2$ peak under the alumina condition, no significant differences were observed among the three types of fillers. In the 25°–55° region the HA and alumina crystals or amorphous silica did not show any change with curing.

The phase change characteristics occurring during the hydration process were similar regardless of the type of filler; however, the expansion deformation was different. To

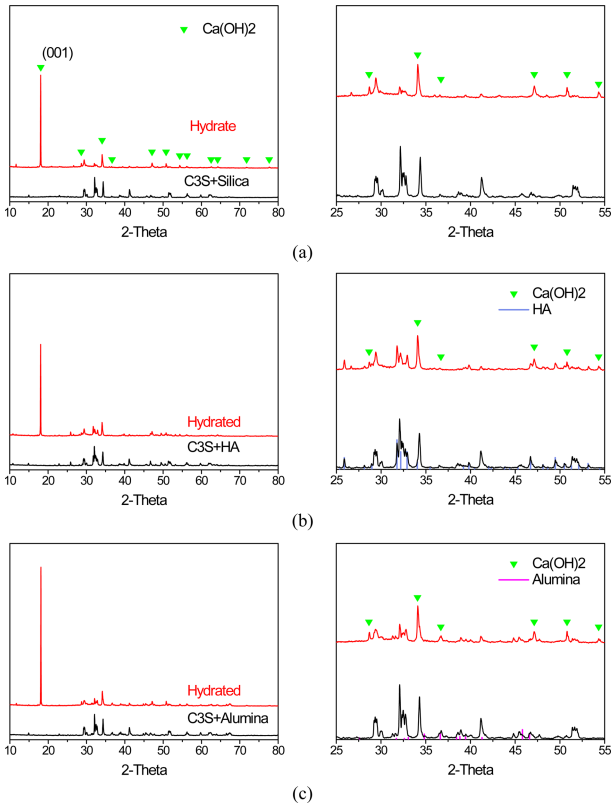

Fig. 6. X-ray diffraction analysis results for hydrated scaffolds with different filler materials: (a) silica with 600 nm diameter, (b) HA, and (c) alumina

compare the hydrate microstructures, the porosity of the scaffold and density of the skeleton were measured using a mercury porosimeter. The differences in density are shown in Fig. 7(a), but the density changes are not in accordance with the expansion phenomenon. The porosity and average pore size of these hydrates follow the order alumina > silica > HA, showing tendencies similar to those of the compressive strength (Figs. 7(b) and (c)). Conditions such as the amount of water, reaction time, temperature, and mixing ratio of the raw materials are known to affect the formation of the hydrate microstructures in hydraulic materials, and the microstructure of a material is a major factor determining its mechanical properties. The similarity between the tendency of the compressive strength of the scaffold hydrate and those of the porosity and pore size means that the hydration reaction of C3S can be controlled by adjusting the type of filler.

To compare the microstructures of the hydrates, the surfaces and fracture surfaces of the scaffolds were observed via SEM. As shown in Fig. 8, the three types of scaffolds exhibit different structures. The plate-shaped and rod-type particles appearing in this figure are all $Ca(OH)_2$ crystals [9]. Plate-shaped particles are observed in the case of silica and HA filler, and rods are found in the case of using HA and alumina. In the silica filler, the small plate-shaped particles are evenly distributed, but they prevent densification of the base material, forming a loose microstructure. Under the HA condition, relatively large plate-like particles are evident and densely packed. Because this microstructure is similar to that of a composite material using plate-shaped particles as fillers, it is presumed that this structural form can express the highest strength among the considered cases. When alumina is used as a filler, the fine particles seem to maintain the highest density, but cracks due to volume expansion were observed on the surface, and the most rod-shaped $Ca(OH)_2$ was found.

Next, the factors affecting the hydration reaction were investigated, as C3S curing starts by reacting with water. An anhydrous slurry was used in this study, and the hydration reaction was induced by immersing the print in a water bath. For the scaffold to harden, it was necessary for the water molecules to diffuse into the print body. The fact that the filler, which did not participate in the chemical reaction of C3S, affected the expansion and microstructure of the scaffold during the hydration process indicated that the characteristics of the filler material were the main factors inducing the diffusion of water molecules.

In a previous study, the mixing of C3A, which had a fast hydration reaction rate, suppressed the expansion of hydrates and made it possible to obtain a well-hydrated and hardened scaffold [8]. Although the fillers used in this study were all inert materials, they stably cured C3S prints, and among them, silica and HA were effective. This finding indicates that the hydrophilicity or wettability of the filler affected the hydration reaction.

Regarding the water curing of C3S, it has been reported that powders such as HA, alumina, and silica can change the microstructure and strength of C3S hydrates, but the cause has not been clearly explained [10-13]. However, one of the results confirmed in those studies is that the mixing of fillers affects the hydration reaction rate of C3S, which is similar to the phenomenon shown in this study. Although different fillers were selected, the hydration reaction rate was

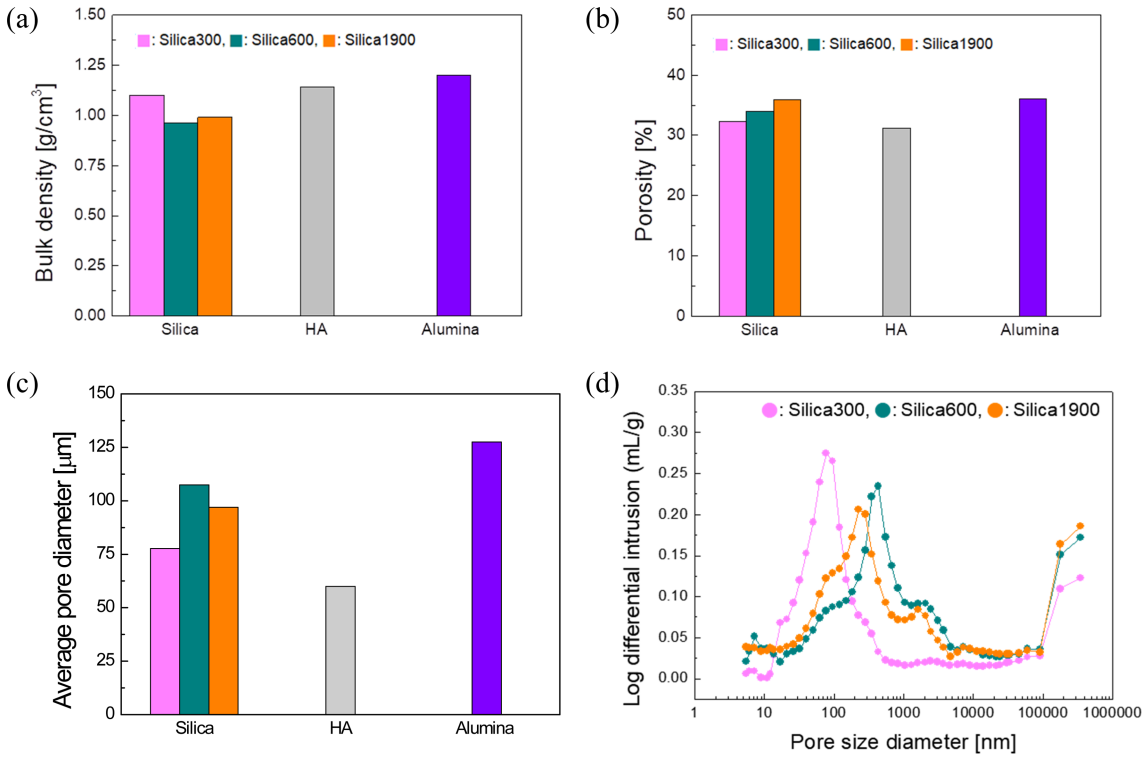

Fig. 7. Mercury porosimeter analysis results for scaffold hydrate: (a) density, (b) porosity, (c) average pore diameter, and (d) pore size distribution with different sizes of silica filler

measured and compared in all of these studies, and it was confirmed that the mixing of the fillers affects the hydration reaction rate of C3S. These results can be said to be similar to the phenomena shown in this study.

The fact that inert material can affect the hydration reaction of C3 means that interactions exist between these substances and water molecules. The reason that an inert material affects the hydration of C3 is because there is an interaction between the material and water molecules. As is well known, different types and sizes of particles have different surface charges, which determine the wettability of solvents [14-15]. In this study, the scaffold blended with silica or HA showed stable reaction characteristics compared to the alumina mixture. All of the filler types showed similar absolute values of surface charge under neutral conditions (pH 7), but as the pH increased, the surface charge of alumina decreased to zero and the surface charge of silica and HA increased in a negative direction [16-18]. Since the hydration of C3S produces $Ca(OH)_2$, the vicinity of the scaffold reached a high pH as the reaction time elapsed, and the wettability of silica and HA increased. A filler with a high absorption rate induces the rapid diffusion of water molecules into the print body, and accelerates the hydration of C3S. The reaction rate also affects the crystal growth of the $Ca(OH)_2$ product. Among these filler materials, HA converted the printed materials into high-strength scaffolds, because hydrates with dense structures were formed while growing plate-like $Ca(OH)_2$ to a uniform and well-packed size.

3.4 Size effect of silica filler in hardening

To check the effect of the filler size on the curing of the scaffold, the support was printed using three types of silica powder, with particle sizes of 300, 600, and 1700 nm. During the hydration process, these scaffolds showed different strains depending on the filler size; however, the scaffolds exhibiting the greatest changes had expansion rates <2.5% (Table 1). Although the deformation was not large, the strength change of the scaffold was notable: the larger the filler particles, the lower the measured compressive strength (Fig. 5). When 300 nm silica was used, the hydrate density was relatively high, porosity was low, and pore size was small (Fig. 7). The smaller the particle size, the greater the

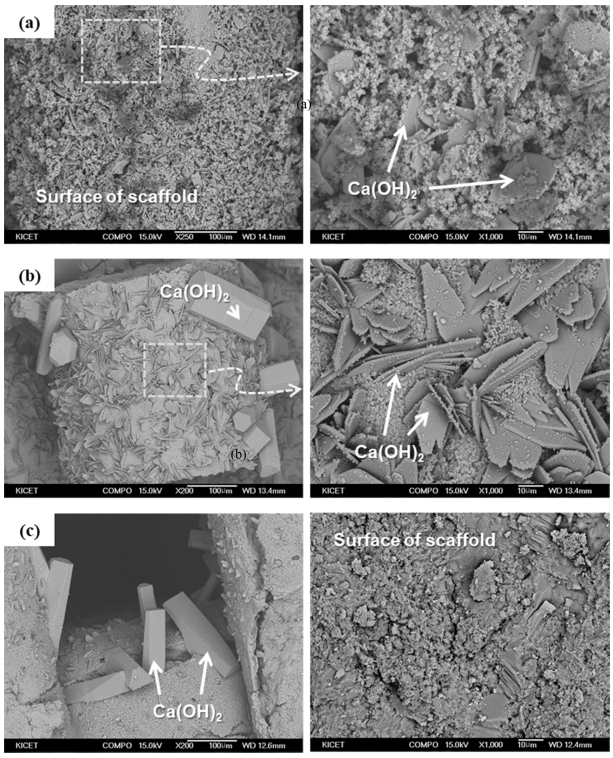

Fig. 8. Surface images of fractured scaffold after hydration reaction with different filler conditions: (a) silica with 300 nm diameter, (b) HA, and (c) alumina

specific surface area. Hence, water molecules could be diffused quickly into the print and water could be supplied effectively to the surrounding C3S particles. Therefore, the curing rate of C3S was increased and a high-density structure with smaller pores was formed, compared to when a filler with a large particle size was used. Hence, this microstructure helped improve the mechanical properties.

4. CONCLUSION

This paper presents a printing method for hydraulic materials using C3S, a representative hydraulic material, and describes the deformation characteristics that occur during the hydration process of printed matter. Silica, HA, and alumina, which do not affect the reaction of C3S, were selected as fillers, and their effects on the shape and mechanical properties of the printed matter were investigated. A support with dimensions of $10.5 \times 10.5 \times 10.14$ (mm) was printed using the FDM method, and a hydrated scaffold was obtained through a two-step curing process.

The scaffolds showed different expansion rates depending on the type of filler; among them, the silica and HA fillers produced the smallest expansion. HA formed a relatively dense hydrate and, as a result, showed the highest compressive strength. Therefore, the acceleration of the hydration reaction rate of C3S can be considered the most important factor for obtaining a hydrate with a low strain rate and high density. In this case, the filler material facilitated the diffusion of water molecules. In addition, a filler with a large specific surface area was advantageous for promoting hydration, compared to a filler with large particles.

An important issue in AM technology is precise printing. Deformation of the size or shape during post-processing is one of the main reasons hindering the development of printed ceramic materials. Knowing that the non-reactive filler can control the moisture diffusion conditions and suppress expansion deformation during hydration, it is expected that application fields of hydraulic materials with complex compositions, such as biocement, can be expanded. However, it will be necessary to study the effects of microstructural changes that happen during the hydration process, and to study the stability of the method of correcting the hydrate and its size.

ACKNOWLEDGEMENT

This research was financially supported by the Institute of Civil Military Technology Cooperation funded by the Defense Acquisition Program Administration and Ministry of Trade, Industry, and Energy of the Korean government under grant No. 21-CM-CE-03. This study was supported by the Korea Institute of Ceramic & Engineering under grant No. KCS19010-1.

REFERENCES

1. Z. Ding, W. Xi, M. Ji, X. Li, Q. Zhang, and Y. Yan, *J. Phys. Chem. Solids* **150**, 109825 (2021).
2. C. Fernández and M. Mercedes, “Effect of particle size on the hydration kinetics and microstructural development of tricalcium silicate” (2008). Ph D Theses, E´cole Polytechnique Fe´de´rale de Lausanne(EPFL). (DOI: 10.5075/epfl-thesis-4102)

3. 3. W. -N Li, J. Chang, Y. –Q. Zhu, and M. Zhang, *Int. Endod. J.* **44**, 41 (2011).
4. 4. A. Cuesta, J. D. Zea-Garcia, D. Londono-Zuluaga, A. G. Torre, I. Santacruz, O. Vallcorba, M. Dpiaggi, S. G. Sanfélix, and M. A. G. Aranda, *Sci. Rep.* **8**, 8544 (2018).
5. 5. C. Yang, X. Wang, B. Ma, H. Zhu, Z. Huan, N. Ma, C. Wu, and J Chang, *ACS Appl Mater Interfaces* **9**, 5757 (2017).
6. 6. W. Wu, W. Liu, J. Jiang, J. Ma, G. Li, J. Zhao, D. Wang, and W. Song, *J. Non-Cryst. Solids* **503**, 334 (2019).
7. 7. P. Pei, D. Wei, M. Zhu, X. Du, and Y. Zhu, *Micropor. Mesopor. Mater.* **214**, 11 (2017).
8. 8. Y. Koo, M. H. Lee, S. Y. Yoon, and Y. Lee, *Korean J. Met. Mater.* **60**, 321 (2022).
9. 9. M. G. Margalha, A. S. Silva, M. R. Veiga, J. Brito, R. J. Ball, and G. C. Allen, J. Mater. Civ. Eng. **25**, 1524 (2013).
10. 10. R. -J. Chung, C. -Y. Lin, P. -Y. Shin, F. -I. Chou, and T. -S. Chin, *J. Med. Biol. Eng.* **23**, 199 (2003).
11. 11. L. P. Singh, S. K. Bhattacharyya, S. P. Shah, G. Mishra, and U. Sharma, *Constr. Build. Mater.* **102**, 943 (2016).
12. 12. J. –B. Zhang, Q. Wang, L. Lu, and Z. –R. Ma, *2nd Int. Semin. Appl, Physics, Optoelectron. Photonics (APOP 2017)*, 507-512.
13. 13. B. Y. Lee, and K. E. Kurtis, *J. Am. Ceram. Soc.* **93**, 3399 (2010).
14. 14. S. Taqvi, and G. Bassioni, "Understanding Wettability through Zeta Potential Measurements." *Wettability and Interfacial Phenomena-Implications for Material Processing* (2019). (DOI: 10.5772/intechopen.84185)
15. 15. I. Mohammed, D. A. Shehri, M. Mahmoud, M. S. Kamal, and O. S. Alade, *ACS Omega* **6**, 12841 (2021).
16. 16. H. Siege, M. Winterer, H. Mühlenweg, G. Michael, and H. Hahn, *Chem. Vap. Deposition* **10**, 71 (2004).
17. 17. C. Wu, L. Wang, D. Harbottle, J. Masliyah, and Z. Xu, *J. Colloid Interface Sci.* **449**, 399 (2015).
18. 18. Y. M. Z. Ahmed, S. M. El-Sheikh, and Z. I. Zaki, *Bull. Mater. Sci*. **38**, 1807 (2015).